Interactions of Organics within Hydrated Selective Layer of Reverse Osmosis Desalination Membrane: a Combined Experimental and Computational Study

Aziz Ghoufi[1], Emil Dražević [2,3*], and Anthony Szymczyk[4]*

[1]*Université de Rennes 1, Institut de Physique de Rennes (UMR CNRS 6251), 263 Avenue du Général Leclerc, CS 74205, 35042 Rennes, France*

[2]*Faculty of Chemical Engineering and Technology, Department of Physical Chemistry, Marulicev trg 19, 10000 Zagreb, Croatia*

[3] *Aarhus University, Department of Engineering, Hangøvej 2, 8200 Aarhus, Denmark*

[4]*Université de Rennes 1, Institut des Sciences Chimiques de Rennes (UMR CNRS 6226), 263 Avenue du Général Leclerc, CS 74205, 35042 Rennes, France*

*corresponding authors

e-mail: anthony.szymczyk@univ-rennes1.fr ; edrazevic@eng.au.dk

Abstract

In this work we have examined a computational approach in predicting the interactions between uncharged organic solutes and polyamide membranes. We used three model organic molecules with identical molecular weights (100.1 g/mol), 4-aminopiperidine, 3,3-dimethyl-2-butanone (pinacolone) and methylisobutyl ketone for which we obtained experimental data on partitioning, diffusion and separation on a typical seawater reverse osmosis (RO) membrane.

The interaction energy between the solutes and the membrane phase (fully aromatic polyamide) was computed from molecular dynamics (MD) simulations and the resulting sequence was found to correlate well with the experimental rejections and sorption data. Sorption of the different organic solutes within the membrane skin layer determined from attenuated total reflection Fourier transform infrared spectroscopy (ATR-FTIR) nicely agreed with interaction energies computed from molecular simulations. Qualitative information about solute diffusivity inside the membrane was also extracted from MD simulations while ATR-FTIR experiments indicated strongly hindered diffusion with diffusion coefficients in the membrane about 10^{-15} m^2/s. The computational approach presented here could be a first step toward predicting rejections trends of e.g. hormones and pharmaceuticals by RO dense membranes.

TOC Art

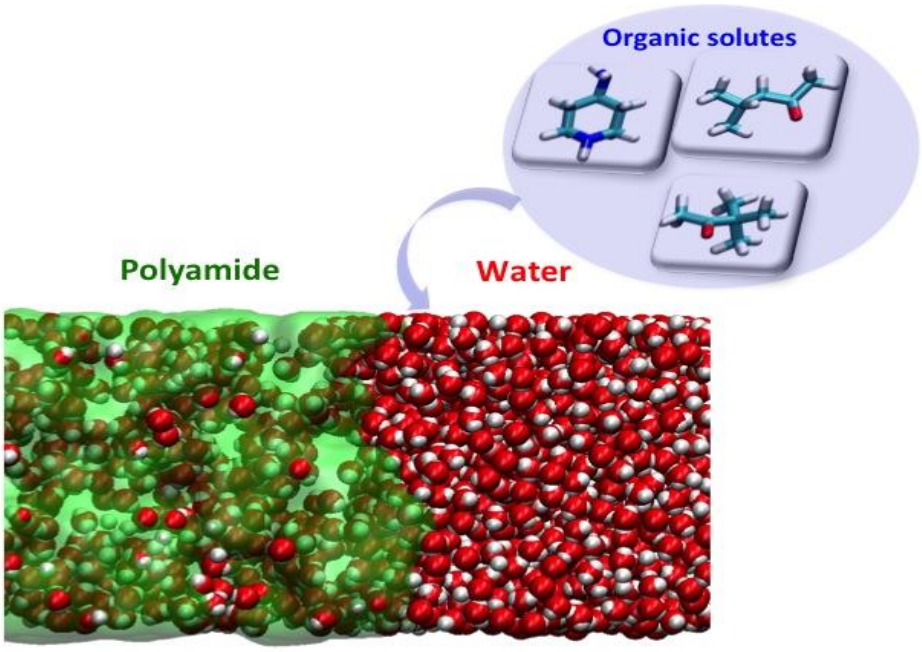

1. Introduction

Reverse osmosis (RO) is a well-established membrane process that is usually used to separate dissolved salts and small organic molecules. Its applications range from the production of ultrapure water for semiconductor and pharmaceutical use to seawater desalination for drinking water production and the purification of industrial wastewater.[1]

Nowadays, the RO and nanofiltration (NF) membrane market is dominated by thin-film-composite polyamide membranes containing three layers: a polyester web serving as the structural support (100-200 μm thick), a mesoporous polysulfone film acting as the supporting mid-layer (about 30-50 μm thick), and a selective ultra-thin skin layer on the upper surface (20-300 nm thick). This latter is generally fabricated through interfacial polymerization of meta-phenylene diamine (MPD) and trimesoyl chloride (TMC) at the interface of two immiscible solvents.[2] These two monomers can react to form linear chains as well as undergo two additional side reactions where the third acyl chloride group can either undergo hydrolysis to form carboxylic acid or react with another diamine molecule to produce cross-linking.[3]

Despite the technological success and importance of both RO and NF, the molecular mechanisms of water and solute transport through RO/NF membranes are not completely understood.[4-6] State of the art is that the rejection of organics is governed by steric, electrostatic (Donnan) and other interaction mechanisms. When organic solute is dissolved at a pH lower than the pKa value of its most acidic group, or at a pH higher than the pKb of its most basic group, it is considered uncharged and thereby the Donnan exclusion mechanism does not apply.

This was well documented in the literature.[6,7-9] Things can be further complicated since solute is excepted to have different pKa and pKb values in bulk water and in the membrane phase (due to extreme confinement). Such behavior was documented in the literature where it was found that carboxylic groups groups in a PA membrane have two pKa values, which was related to two different types of voids, and thus environments[10], so significant variations can be expected, depending on the membrane structure. Although the steric exclusion is the dominating mechanism for an uncharged organic, specific solute-membrane interactions allow can affect adsorption, and thus partitioning and diffusion through the active layer of the RO/NF membranes, which affects rejection.[11-14] This was further explored during the recent years and it has been shown that significant amounts of hormones and phenolic compounds adsorb strongly in and on the selective layer of NF polyamide based membranes.[15,16] Moreover, Verliefde et al. showed that by including the solute-membrane interactions in a very simple pore flow model one can estimate the rejection of uncharged organics with NF membranes reasonably well.[17] Several other studies showed that rejection of uncharged organic solutes by RO membranes cannot be described by a simple sieving effect ruled by the relative size of the solutes and the free volumes within the membrane active layer.[18-20] These works also highlighted the crucial role of physicochemical interactions between organic solutes and the membrane material. However, understanding solute / membrane interactions is extremely challenging from an experimental point of view because RO membranes are essentially thin-film composite materials, where the skin layer does not represent more than ~ 0.1 % of the total membrane thickness. One of the pathways to understand the fundamentals that lay behind solute-membrane interactions is to pair state of the art experimental and theoretical approaches. Electrochemical impedance spectroscopy (EIS) has proved to be an attractive technique to investigate both solute partitioning and diffusion in membrane skin layers.[18] However, the EIS-based method is restricted to electroactive solutes. Another method based on attenuated total

reflection Fourier transform infrared spectroscopy (ATR-FTIR) was proposed to determine partitioning inside thin films.[21] Fieldson and Barbari showed that ATR-FTIR could also be used to gain insight into solute diffusion inside polymer films.[22] Their method was recently applied by Dražević et al. who reported the first measurements of organic solute diffusion inside the skin layer of a RO membrane.[19] It should be stressed that both methods, EIS and ATR-FTIR, have to be applied to the free-standing membrane skin layer. This requires separating this latter from the rest of the membrane, which can be done by selective dissolution of membrane sublayers.[23]

We have therefore used ATR-FTIR spectroscopy and molecular dynamics (MD) simulations to estimate diffusion, partitioning an interaction energies of three model organic solutes (4-aminopiperidine, 3,3-dimethyl-2-butanone (pinacolone) and methylisobutyl ketone), with identical molar mass (100.1 g/mol). The interaction energy between model organics and the hydrated polyamide polyamide layer was computed from MD and compared to partitioning coefficients obtained experimentally from ATR-FTIR spectroscopy.

2. Computational Details

The organic solutes (see chemical structures in Figure 1) and the polyamide (PA) membrane skin layer were modeled by means of the AMBER force field.[24] Structural information of the PA membrane skin layer can be found elsewhere.[25,26] A cutoff radius of 12 Å was set for both electrostatic and van der Waals interactions. The electrostatic contribution was computed by using the Ewald sum method with a convergence parameter of 0.24 $Å^{-1}$ while the van der Waals interactions were modeled by means of the Lennard-Jones (LJs) potential. Crossed LJs interactions between atoms of PA and those of organic solutes were evaluated from the Lorentz-Berthelot mixing rule. Water molecules were described by the TIP4P/2005 model.[27]

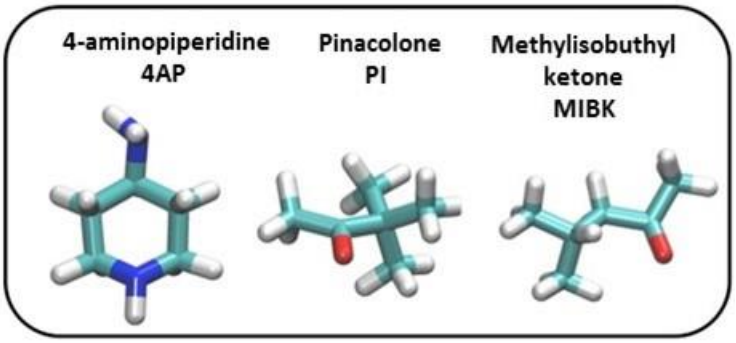

Figure 1. Chemical structures of the organic solutes considered in this work. Carbon, hydrogen, nitrogen and oxygen atoms are shown in light blue, white, navy blue and red, respectively.

In order to reproduce the hydration process of the PA membrane two reservoirs containing 4600 water molecules and 20 solute molecules were added on each side of the dry membrane (see Figure S1 in the supporting information). In the initial configuration organic solutes were inserted close to the membrane surface in order to decrease the computational time. Two graphene walls were also added on each side of the simulation box. After an equilibration in the canonical ensemble (NVT where N is the number of particles, V the volume and T the temperature) at 300 K (see SI for details), non-equilibrium molecular dynamics (NEMD) simulations were performed by applying an external force on each atom of the graphene walls (thus acting as pistons forcing water molecules and organic solutes to enter the PA membrane) so that the external pressure acting on the system was equal to 1 bar. Once a stationary regime was reached, i.e. when the water content inside the membrane became constant (see Results and Discussion section), the force applied on the graphene walls was shut down and equilibrium MD simulations were performed in the NP_nT statistical ensemble[28] (5 ns of equilibration followed by an acquisition phase of 10 ns). Temperature (T) and normal pressure (P_n) were kept constant and equal to 300 K and 1 bar, respectively, by means of the Nose-Hoover algorithm[29] with relaxation times of 0.1 and 0.5 ps for the thermostat and the anisotropic barostat, respectively.

Additional equilibrium MD simulations of the different organic solutes in bulk water (1000 water molecules and 5 solute molecules) were carried out for comparison with results obtained inside the membrane.

Both equilibrium and non-equilibrium MD simulations were carried out with DL_POLY software.[30] Integration of the equations of motion was performed by means of the velocity Verlet algorithm[31] with a time step of 1 fs.

Mean Square Displacement (MSD) was computed by using the following correlation equation:

$$MSD(t) = \langle \frac{1}{N} \sum_{i=1}^{N} (\boldsymbol{r}_i(t) - \boldsymbol{r}_i(0))^2 \rangle \quad (1)$$

where $\mathbf{r}_i(t)$ denotes the position of a particle *i* at time *t* and N the number of particles.

3. Experimental

Membrane and chemicals

Desalination membrane SWC4+ (Hydranautics/Nitto Denko, Oceanside, CA, USA) was used in this work as a representative RO membrane with the chemistry of fully aromatic polyamide (PA). Methylisobutyl ketone (Fluka, puriss. ACS; p.a. >99% (GC)), pinacolone (Aldrich, 98%) and 4 aminopiperidine (Tokyo Chemical Industry Co. LTD, > 95 %) were used without further purification. It should be noted that all these three compounds have identical molar mass (100.1 g/mol).

Equilibrium partitioning and diffusion measurements

Solutions were prepared in the range of concentrations 0.1 – 0.5 mol/L, depending on the solubility of a particular solute in water. Stacks of five SWC4+ skin layers were isolated on the ATR crystal using the same procedure that was described elsewhere.[32] Thickness of individual SWC4+ layers along with stacks of layers in dry and wet state may be found elsewhere.[19]

Equations and the numerical procedure for estimating the molar extinction coefficients were described in details elsewhere.[21,22] Main equations along with some experimental data can be found in the SI. Experimentally obtained molar extinction coefficients are presented in Table 1.

Table 1. Molar exctinction coefficients, obtained using FTIR on bare diamond, T=21°C.

Solute	ε/m^{2}mol^{-1}
4 aminopiperidine	19.8
Pinacolone	94.8
Methylisobutyl ketone	112

All infrared spectra were recorded at a rate of 1.64 second per spectrum at a resolution of 2 cm^{-1} in the range 400 - 4000 cm^{-1} using a Bruker Vertex 70 series FTIR spectrometer equipped with a Bruker Platinum ATR accessory with a single reflection diamond crystal (n_d=2.4). Temperature in the room was held constant at 21°C, with the use of air conditioning device.
A stainless steel liquid cell (PikeTech ATR Flow-Through Attachment) was mounted on top of the crystal to enclose the polyamide films, and diffusion measurements were performed using the following procedure;

1) Deionized water was injected into the liquid cell using a stainless steel syringe,
2) A sequence of spectra was recorded until no change was observed to verify the PA film was equilibrated with water,
3) After equilibrium with water was reached, the spectrum of PA film in water was recorded as the background for subsequently recorded spectra,
4) A solution of a particular organic solute was injected and a sequence of spectra over time was recorded to monitor the change of the appropriate solute band.

All measurements were repeated at least three times for each solute, each time with a freshly prepared stack of PA layers. Equilibrium absorbance and diffusion coefficient were estimated by fitting Equation S7 given in the supporting information.

Rejection experiments

The RO setup used in this study is depicted in Fig. 2 and described in details elsewhere.[32] Briefly, SWC4+ membrane was initially soaked in a 1:1 water:ethanol solution, rinsed with deionized water and then placed in the reverse osmosis cell. The membrane was further pressurized with Milli-Q water at 40 bar for two hours. Milli-Q water was drained from the system and five liters of 2.5 mmol/L solutions were circulated through the system for 8 hours in order to saturate the membrane with a given solute before the rejection measurements. Measurements were performed at a constant temperature of 21.0 ± 0.1 °C. RO measurements were performed at transmembrane pressure differences of 11, 13, 15 and 17 bar. Concentrations in feed (C_f) and permeate (C_p) were measured using Shimadzu TOC-VWS Carbon Analyzer.

Permeate flux was determined by weighing the permeate as a function of time. Rejection (R) of each solute was calculated using:

$$R = 1 - \frac{C_p}{C_f} \quad (2)$$

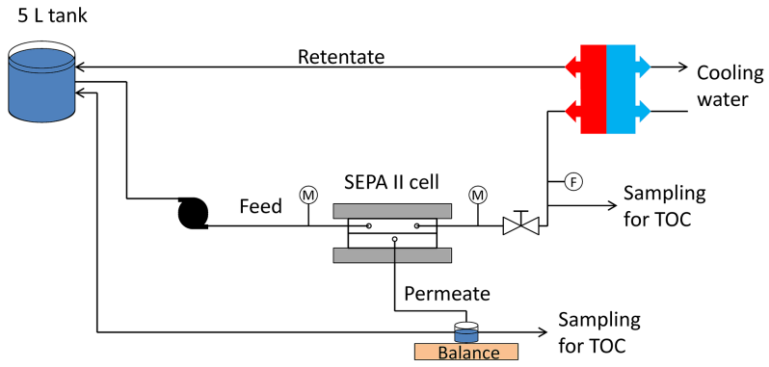

Figure 2. RO setup used in this study. Symbols M stand for manometer and F for flowmeter. Feed was circulated at constant flow rate in closed loop system at constant temperature and different pressures.

4. Results and discussion

Figure 3 shows the experimental solute rejections by the SWC4+ membrane as a function of the permeate flux. All the three organics were found to be strongly rejected by the membrane (R > 0.95) with the sequence 4 aminopiperidine (4AP) > pinacolone (PI) > methylisobutyl ketone (MIBK). The phenomena that control the separation performance of RO membranes occur inside subnanometric free volumes between the polymer chains.[3,33] Molecular simulations were then carried out to rationalize these phenomena. An all-atom model of a PA membrane that has been shown to be fairly representative of actual RO membranes[25,26,34] was used in this work. As mentioned in section 2, the dry PA membrane was connected with two reservoirs containing water and organic solute molecules, and was further hydrated by running a non-equilibrium MD simulation. The time evolution of the membrane water content is shown

in Figure 4. Since there was no perfectly defined membrane/water interface water molecules were considered to be inside the membrane when located where the PA density was found almost constant, i.e. for z between – 42 and + 42 Å (see Fig. S2 in the SI). The number of water molecules entering the membrane increased rapidly before levelling off, leading to water content close to 24 wt% independently of the organic solute added to water. This relatively high water uptake is in good agreement with experimental results[3,35] and has been shown to result from favorable interactions between PA and water molecules that compensate the energetic penalty associated with the loss of hydrogen bonds formed between water molecules inside the PA membrane.[26]

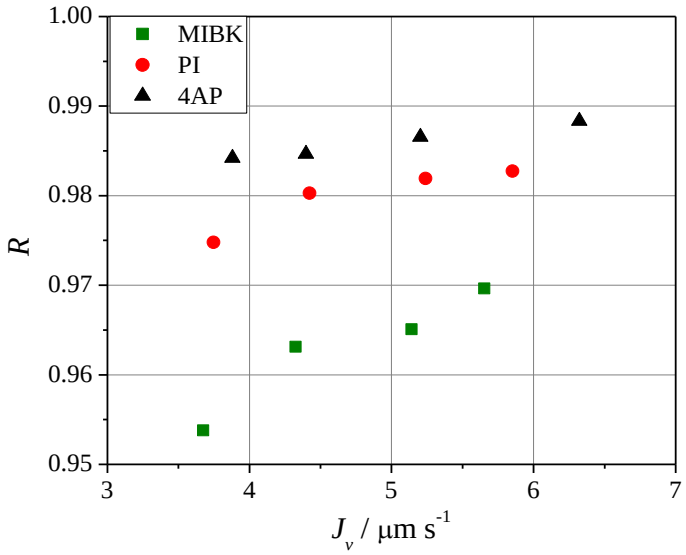

Figure 3. Experimental rejection of organic solutes by SWC4+ membrane as a function of the permeate volume flux.

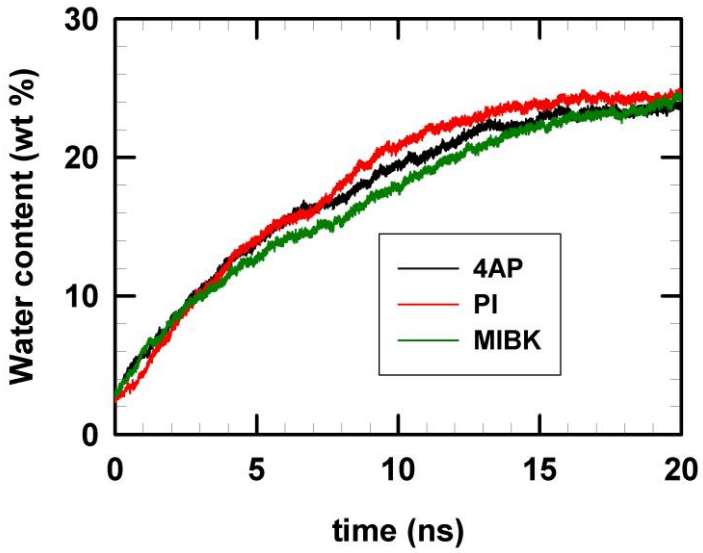

Figure 4. Time evolution of water content inside the PA membrane during the hydration process in the presence of the different organic solutes.

After completion of the hydration process an MD simulation at equilibrium (no external force applied on the system) was performed so as to determine the interaction energy between the different components (water, organic solute and membrane). Figure 5 shows the difference between the interaction energy (including both Lennard-Jones and electrostatic contributions) of the organic solutes inside the membrane phase and in bulk water (ΔE). Simulation results correlate qualitatively with experimental rejections (Figure 3) since a more negative ΔE is associated with a lower solute rejection.

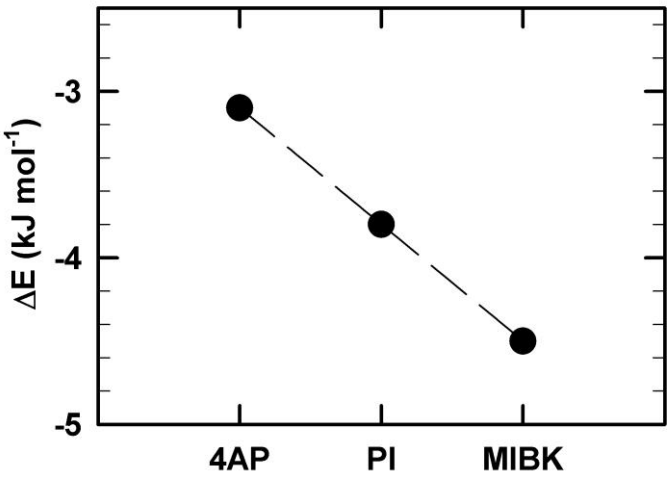

Figure 5. Difference between the interaction energy of the organic solutes and the membrane phase and the interaction energy of the organic solutes and bulk water.

The sequence of relative solute affinity for the PA membrane phase was also corroborated by ATR-FTIR spectroscopy performed with stacks of isolated skin layers of SWC4+ membrane. Indeed, as shown in Table 2 the lowest and highest partitioning coefficients (defined as the ratio between the solute concentration in the PA film and that in the external solution) were obtained with 4 aminopiperidine (4AP) and methylisobutyl ketone (MIBK), respectively.

Table 2. Partition coefficients (*K*) of the organic solutes estimated from FTIR spectroscopy.

Solute	4AP	PI	MIBK
K(exp. 1)	0.69	0.52	1.38
K(exp. 2)	0.52	0.58	3.16
K(exp. 3)	0.56	0.83	3.51
K(exp. 4)	0.47	0.85	2.72
K(exp. 5)	0.47	0.59	2.75
K (Avg.)	**0.54**	**0.67**	**2.70**
Std. dev.	**0.09**	**0.15**	**0.81**

The different contributions to the interaction energy between the organic solutes and the membrane phase inferred from MD simulations are reported in Figure 6. As expected, the contribution of solute-solute interactions inside the PA membrane was found to be negligible with respect to solute-PA and solute-water contributions. Interestingly, interactions with PA were found more favorable for 4 aminopiperidine than for pinacolone but the opposite was true for the interaction between these solutes and water confined inside the membrane, thus resulting in a stronger overall affinity of pinacolone for the membrane phase with respect to water phase outside the membrane (Figure 5). Pinacolone has one ketone group, which suggests it interacts stronger than 4 aminopiperidine with both water and PA. Indeed, on Pauling electronegativity scale nitrogen atom (3.04) is less electronegative than oxygen atom (3.44), and thus C-N or C-N-C bonds in 4 aminopiperidine are less polar than C=O bond in pinacolone. This is well supported by experimental data, i.e. by the lower rejection of pinacolone and its higher partitioning in PA. Both pinacolone and MIBK have one ketone group. However, the pinacolone's ketone group is "protected" by a bulky tert-butyl group, which makes the interaction of pinacolone with water within PA weaker than that of MIBK (see Fig. 6). Solute-PA interaction trend can be explained in a same manner. In PA both polar and non-polar interactions occur. In comparison to small water molecules, which can to some extent rotate in nanoconfined spaces, and therefore access and interact with both PA and confined solutes, confined organic molecules have very low mobility (lower degree of freedom), which is experimentally supported by very low diffusivity values.[19] It is suggested here that because of low degree of freedom and protective behavior of tert-butyl group, polar interactions between PA and the ketone group of pinacolone were significantly hindered, which could explain weaker pinacolone-PA interaction in Figure 6. Nevertheless, its interaction with water within PA was still significant. This finding highlights the crucial role played by water confined in the PA

matrix and thus the importance of water uptake in the performance of reverse osmosis membranes.

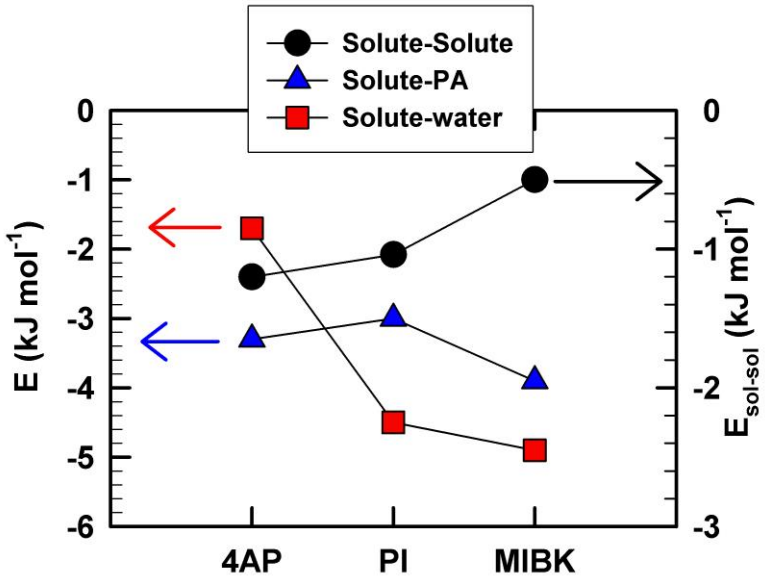

Figure 6. Different contributions to the solute interaction energy in the membrane phase.

In this last part we focused on solute diffusion through the PA membrane since it is commonly accepted that a solution/diffusion mechanism rules transport through RO membranes[36] and then, determining the interaction energies and equilibrium partitioning coefficients might not be enough to fully explain experimental rejections shown in Figure 3. Self-diffusion coefficients can be inferred from equilibrium MD simulations by means of the particle mean square displacement (MSD) and the Einstein relation provided that the MSD varies linearly with time.[37]

Figure 7 shows the time evolution of MSD for the three organic solutes in the PA membrane. Non-linear variations were observed for all solutes. It was then impossible to extract the solute self-diffusion coefficients inside the membrane from MSDs. However, the variation of MSD with time strongly indicates a faster diffusion of methylisobutyl ketone inside the membrane compared with both 4 aminopiperidine and pinacolone. This may be related with the more linear

structure of methylisobutyl ketone while 4 aminopiperidine and pinacolone have cyclic and bulky tert-butyl groups, respectively. These results, together with the difference of interaction energies inside and outside the membrane phase (Figure 5), are then consistent with the rejection sequence observed experimentally (Figure 3).

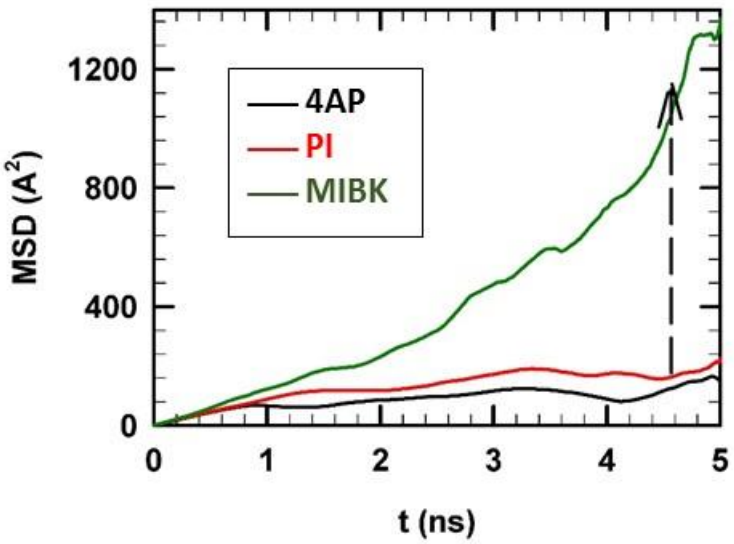

Figure 7. Mean square displacement of the different organic solutes in the PA membrane vs. time.

Finally, we experimentally determined the diffusion coefficients of all three organic within skin layers of the SWC4+ membrane from FTIR spectroscopy according to the experimental procedure described in section 3. By fitting experimental results to Equation S7 of the supporting information extremely small diffusion coefficients, in the order of 10^{-15} m^2/s, were obtained for the three organic solutes (see example in Figure 8). Unfortunately, the experimental error in connection with FTIR experiments was too large to allow us to clearly differentiate among the different solutes. Some of our experimental data suggest that MIBK had lower diffusion coefficient compared to 4AP and pinacolone (Figure S6 and S7). However in the case of pinacolone and 4AP, also MIBK, scattering of data points was very high and it

significantly affected the reproducibility of the diffusion tests. High scattering was related to very low partition coefficients, since because of low partitioning the IR signal in PA became much lower than that in pure water. Scattering was also related to the fact that only one scan had been taken every 1.64 seconds, and it is excepted that reproducibility would have been much higher if FTIR setup was able to make 10 scans every 1 second. For this reason we are only confident to say diffusion coefficients are around 10^{-15} m^2s^{-1}, however it is impossible to resolve whether diffusion of MIBK was indeed lower than that of 4AP and pinacolone neither that 4AP nor pinacolone diffused slower than MIBK.

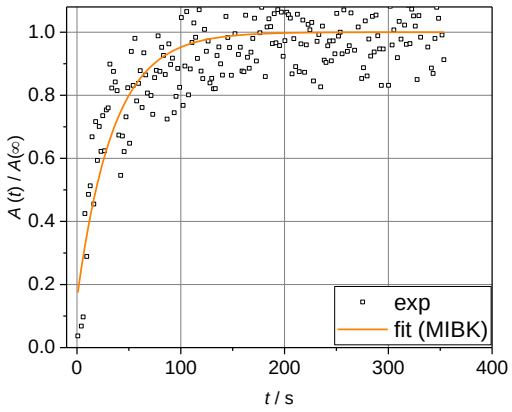

Figure 8. An example showing typical ATR-FTIR data used to extract diffusion coefficient and $A(\infty)$ of MIBK. As an average of five different measurements values were: $A(\infty)$ 0.073 ± 0.002 and D = 2.56.10^{-15} ± 1.43.10^{-15} m^2s^{-1}.

Overall, qualitative diffusivity results and interaction energies determined from molecular simulations and equilibrium partitioning coefficients inferred from ATR-FTIR experiments were consistent with experimental rejections of 4 aminopiperidine, pinacolone and methylisobutyl ketone. Good agreement between molecular simulation and experimental data confirms the relevance of the combined approach which added to the understanding of the separation of organic solutes by dense RO membranes. It has been shown that the total solute-hydrated membrane interaction is governed by both solute-water and solute-polymer interactions. This means that solute-dry polymer affinity predicted using, e.g., Hansen solubility

parameters may not apply simply because it does not account for the water content in RO membranes. It also means that solutes that have high affinity for both polymer and water are expected to have high partitioning in polyamide-based membranes, which agrees well with high partitioning reported earlier for n-alcohols in such membranes.[14]

Supporting Information Available

Computational details; main equations for determination of partitioning coefficients and diffusion coefficients from ATR-FTIR; additional ATR-FTIR results. This information is available free of charge via the Internet at http://pubs.acs.org/.

References

(1) Drioli, E.; Macedonio, F. Membrane Engineering for Water Engineering. *Ind. Eng. Chem. Res.* **2012**, *51*, 10051-10056.

(2) Wang, T.; Dai, L.; Zhang, Q.; Li, A.; Zhang, S. Effects of acyl chloride monomer functionality on the properties of polyamide reverse osmosis (RO) membrane. *J. Membr. Sci.* **2013**, *440*, 48-57.

(3) Lee, J.; Doherty, C.M.; Hill, A.J.; Kentish, S.E. Water vapor sorption and free volume in the aromatic polyamide layer of reverse osmosis membranes. *J. Membr. Sci.* **2013**, *425-426*, 217-226.

(4) Schäfer, A.I.; Akanyeti, I.; Semião, A.J.C. Micropollutant sorption to membrane polymers: a review of mechanisms for estrogens. *Adv. Colloid Interface Sci.* **2011**, *164*, 100-117.

(5) Plakas, K.V.; Karabelas, A.J. Removal of pesticides from water by NF and RO membranes - a review. *Desalination* **2012**, *287*, 255-265.

(6) Bellona, C.; Drewes, J.E.; Xu, P.; Amy, G. Factors affecting the rejection of organic solutes during NF/RO treatment - a literature review. *Water Res.* **2004**, *38*, 2795-2809.

(7) Nghiem, L.D.; Schäfer, A.I.; Elimelech, M. Pharmaceutical Retention Mechanisms by Nanofiltration Membranes. *Environ. Sci. Technol.* **2005**, *39*, 7698-7705.

(8) Nghiem, L.D.; Schäfer, A.I.; Elimelech, M. Role of electrostatic interactions in the retention of pharmaceutically active contaminants by a loose nanofiltration membrane. *J. Membr. Sci.* **2006**, *286*, 52-59.

(9) Bellona, C.; Drewes, J.E. The role of membrane surface charge and solute physico-chemical properties in the rejection of organic acids by NF membranes. *J. Membr. Sci.* **2005**, *249*, 227-234.

(10) Coronell, O.; Gonzalez, M.; Marinas, B.J.; Cahill, D.G. Ionization behavior, stoichiometry of association, and accessibility of functional groups in the active layers of reverse osmosis and nanofiltration membranes. *Environ. Sci. Technol.*, **2010**, *44*, 6808–6814.

(11) Kimura, K.; Amy, G.; Drewes, J.; Watanabe, Y. Adsorption of hydrophobic compounds onto NF/RO membranes: an artifact leading to overestimation of rejection. *J. Membr. Sci.* **2003**, *221*, 89-101.

(12) Nghiem, L.D.; Schäfer, A.I.; Elimelech, M. Removal of natural hormones by nanofiltration membranes: measurement, modeling, and mechanisms. *Environ. Sci. Technol.* **2004**, *38*, 1888-1896.

(13) Nghiem, L.D.; Schäfer, A.I.; Elimelech, M. Nanofiltration of hormone mimicking trace organic contaminants. *Sep. Sci. Technol.* **2005**, *40*, 2633-2649.

(14) Ben-David A;. Oren, Y.; Freger, V. Thermodynamic factors in partitioning and rejection of organic compounds by polyamide composite membranes. *Environ. Sci. Technol.* **2006**, *40*, 7023-7028.

(15) Semião, A.J.C.; Schäfer, A.I. Removal of adsorbing estrogenic micropollutants by nanofiltration membranes. Part A - Experimental evidence. *J. Membr. Sci.* **2013**, *431*, 244-256.

(16) Sotto, A.; Arsuaga, J.M.; Van der Bruggen, B. Sorption of phenolic compounds on NF/RO membrane surfaces: Influence on membrane performance. *Desalination* **2013**, *309*, 64-73.

(17) Verliefde, A.R.D.; Cornelissen, E.R.; Heijman, S.G.J.; Hoek, E.M.V.; Amy, G.L.; Van der Bruggen, B.; Van Dijk, J.C. Influence of solute-membrane affinity on rejection of uncharged organic solutes by nanofiltration membranes. *Environ. Sci. Technol.* **2009**, 43, 2400-2406.

(18) Dražević, E.; Bason, S.; Košutić K.; Freger, V. Enhanced partitioning and transport of phenolic micropollutants within polyamide composite membranes. *Environ. Sci. Technol.* **2012**, 46, 3377-3383.

(19) Dražević, E.; Košutić K.; Kolev, V.; Freger, V. Does hindered transport theory apply to desalination membranes? *Environ. Sci. Technol.* **2014**, 48, 11471-11478.

(20) Dlamini, D.S.; Levchenko S.; Bass, M.; Mamba, B.B.; Hoek, E.M.V.; Thwala J.M.; Freger, V. Solute hindrance in non-porous membranes: an ATR-FTIR study. *Desalination* **2015**, *368*, 60-68.

(21) Freger, V.; Ben-David, A. Use of attenuated total reflection infrared spectroscopy for analysis of partitioning of solutes between thin films and solution. *Anal. Chem.* **2005**, *77*, 6019-6025.

(22) Fieldson, G.T.; Barbari, T.A. The use of FTi.r.-a.t.r. spectroscopy to characterize penetrant diffusion in polymers. *Polymer* **1993**, *34*, 1146-1153.

(23) Freger, V. Swelling and morphology of the skin layer of polyamide composite membranes: an atomic force microscopy study. *Environ. Sci. Technol.* **2004**, 38, 3168-3175.

(24) Cornell, W.D.; Cieplak, P.; Bayly, C.I.; Gould, I.R.; Merz, K.M.; Ferguson, D.M.; Spellmeyer, D.C.; Fox, T.; Caldwell, J.W.; Kollman, P.A. A second generation force field for the simulation of proteins, nucleic acids, and organic molecules. *J. Am. Chem. Soc.* **1995**, *117*, 5179-5197.

406 (25) Ding, M.; Szymczyk, A.; Ghoufi, A.; Goujon, F.; Soldera, A. Structure and dynamics of
407 water confined in a polyamide reverse-osmosis membrane: a molecular-simulation study. *J.*
408 *Membr. Sci.* **2014**, *458*, 236–244.
409 (26) Ding, M.; Szymczyk, A.; Ghoufi, A. Hydration of a polyamide reverse osmosis membrane.
410 *J. Membr. Sci.* **2016**, *501*, 248–253.
411 (27) Abascal, J. L.; Vega, C. A general purpose model for the condensed phases of water:
412 TIP4P/2005. *J. Chem. Phys.* **2005**, *123*, 234505.
413 (28) Ghoufi, A.; Morineau, D.; Lefort, R.; Hureau, I.; Hennous, L.; Zhu, H.; Szymczyk, A.;
414 Malfreyt, P.; Maurin, G. Molecular simulations of confined liquids: an alternative to the GCMC
415 simulations. *J. Chem. Phys.* **2011**, *134*, 074104.
416 (29) Nosé, S. A unified formulation of the constant temperature molecular dynamics methods.
417 *J. Chem. Phys.* **1984**, *81*, 511-519.
418 (30) Todorov, I.; Smith, W.; Trachenko, K.; Dove, M. DL_POLY_3: new dimensions in
419 molecular dynamics simulations *via* massive parallelism. *J. Mater. Chem.* **2006**, *16*, 1911-1918.
420 (31) Swope, W.C.; Andersen, H.C.; Berens, P.H., Wilson, K.R. A computer simulation method
421 for the calculation of equilibrium constants for the formation of physical clusters of molecules:
422 application to small water clusters. *J. Chem. Phys.* **1982**, *76*, 637-649.
423 (32) Dražević, E.; Košutić, K., Freger, V. Permeability and selectivity of reverse osmosis
424 membranes: correlation to swelling revisited. *Water Res.* **2014**, *49*, 444-452.
425 (33) Singh, P.S.; Ray, P; Xie, Z.; Hoang, M. Synchrotron SAXS to probe cross-linked network
426 of polyamide 'reverse osmosis' and 'nanofiltration' membranes. *J. Membr. Sci*. **2012**, *421-422*,
427 51-59.
428 (34) Ding, M.; Ghoufi, A.; Szymczyk, A. Molecular simulations of polyamide reverse osmosis
429 membranes. *Desalination* **2014**, *343*, 48-53.

(35) Kotelyanskii, M.J.; Wagner, N.; Paulaitis, M. Atomistic simulation of water and salt transport in the reverse osmosis membrane ft-30. *J. Membr. Sci.* **1998**, *139*, 1-16.

(36) Wijmans, J.G.; Baker, R.W. The solution-diffusion model: a review. *J. Membr. Sci.* **1995**, *107*, 1-21.

(37) Allen, M. P.; Tildesley, D. J. *Computer simulation of liquids*. Clarendon press, Oxford, **1987**.